Influence of the Droop and Ripple of Modulator on Klystron Output

R. Zeng, A. J. Johanssan, K. Rathsman, S. Molloy

September 15, 2011

Abstract

The variations of the phase and amplitude of klystron output due to the change in klystron cathode voltage is investigated in this note. The mechanism and the effectiveness of the feedback control to suppress the variations are given. To understand the limitation of the feedback, both proportional controller and proportional-integral controller used in feedback loop are simulated and analyzed respectively for superconducting cavity and normal conducting cavity. The tolerances of the droop and ripple in cathode voltage are shown according to the data and results obtained. All the simulations and calculations are performed with MATLAB. The data and results are listed in detail so as to enable comparison with further studies and measurements at ESS.

1 Introduction

In accelerator, the klystron suffers the droop and ripple effect resulting from the modulator (klystron cathode voltage supplier), while the droop and ripple in klystron cathode voltage leads to a phase and amplitude modulation on klystron output. At ESS, there might be potentially serious droop and ripple because of long pulse up to 3 ms. It is important for us to know to what extent the droop and ripple affects the klystron output, and how much we can tolerate.

2 Phase and Amplitude Variations

To find how the klystron output is affected, consider a simplified two-cavity klystron as shown in Figure 1.

Electron beams generated out from Electron gun are firstly accelerated by the cathode voltage V and then modulated by the RF signal at input cavity. After passing through the drift space of the length L, the beams finally induce the required RF signal at output cavity. The RF output phase varies if there is any change in the time to travel through the drift space, which is highly affected by the change in cathode voltage. The phase variation due to the voltage change can be calculated by the following equations:

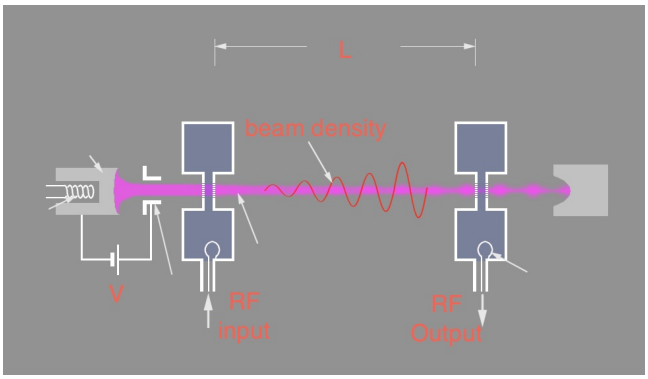

Figure 1: Two-cavity klystron schematic diagram [1]

$$t = \frac{L}{v} = \frac{L}{\sqrt{\frac{eV}{m}}}, \tag{1}$$

$$\theta = \omega t, \tag{2}$$

$$d\theta = -\frac{\omega L}{\sqrt{\frac{2eV}{m}}}\frac{dV}{V}, \tag{3}$$

where v is the velocity of the beam, V is the cathode voltage of klystron, L is the length between the RF input and output of klystron, t is the time delay of the beam for a L length travelling, θ is the corresponding phase delay with RF frequency ω, $d\theta$ is the phase variation, dV is the voltage variation and e/m is the charge to mass ratio of an electron. More accurate result can be calculated by the relations given in Appendix A [2] in consideration of relativistic effects.

There is also variation in amplitude as a result of the change in klystron cathode voltage. The calculation of the amplitude variation [3] is based on the following relations:

$$P_{out} \propto V^{5/2}, \tag{4}$$

$$V_{out} \propto P_{out}^{1/2}, \tag{5}$$

$$V_{out} \propto V^{5/4}, \tag{6}$$

$$\frac{dV_{out}}{V_{out}} = \frac{5}{4}\frac{dV}{V}. \tag{7}$$

Assuming that the RF input is $cos(\omega t)$ and there is error ΔV in cathode voltage, the RF output signal is therefore modulated by $\Delta\theta$ in phase and ΔA in amplitude, which can be written as:

$$V_{out} = (A + \Delta A)cos(\omega t + \Delta\theta), \tag{8}$$

where A is the klystron gain. For example, considering a klystron with $L = 2.5m$, $f = 508MHz$, and the cathode voltage = $80kV$, a cathode voltage change $\Delta V/V = 1\%$ results in a phase variation $\Delta\theta$ of 13° (12° for

relativistic case), and amplitude variation $\Delta A/A$ of 1.25%. Some measurements for the phase and amplitude variations in other labs are listed in Table 1. They are in agreement with the ones calculated above.

Table 1: Measurement for the phase and amplitude variations in other labs

	RF frequency /MHz	Cathode voltage change	Phase variation /deg.	Amplitude variation
JPARC[4]	312	3.40%	25	˜8%(power)
SNS[5, 6]	805	3%	˜50(max)	˜8%(power)
PEPII[7]	476		˜14° /kV	
SACLAY[8]	704.4	200V@95kV	10° /kV@92kV	

It appears that the phase is much more influenced by the ripple than the amplitude. Therefore, we will mainly discuss the phase variations in later sections. If there is ripple component $\Delta V sin(\omega t)$ mixed in cathode voltage, the RF output signal correspondingly become:

$$Acos(\omega t + k\Delta V sin(\omega t)). \tag{9}$$

It is the common expression of the frequency modulated signal, which has been well studied in radio communication. Because the droop can be also viewed as the ripple with DC component or very low frequency component, we will therefore discuss just the case of the ripple components with various frequencies in the following sections.

3 Suppression of variations

The amplitude and phase variations of klystron output resulted from modulator droop and ripple can be suppressed in feedback loop by a factor of G+1, where G is the loop gain. However, the feedback gain G cannot be unlimitedly increased due to the loop delay. The low gain limits the feedback performance and leaves steady errors. The integral gain is then introduced to eliminate the steady error and also the low frequency noises, but have a poor performance at high frequency. More details will be given in following sections.

3.1 Loop delay and loop gain

The block diagram of a simplified feedback loop for cavity phase and amplitude (or I & Q) control is given in Figure 2, where the klystron, cavity and detector are all simulated as the one-order low pass filters [9, 10], and only proportional controller is considered. The loop delay is generally of the order of µs in LLRF system, which is the key factor causing loop instability and limiting loop performance. If we note that the 3-dB cut-off frequencies of the klystron and the detector are usually much higher than the Cavity, the block diagram can be further simplified into Figure 3.

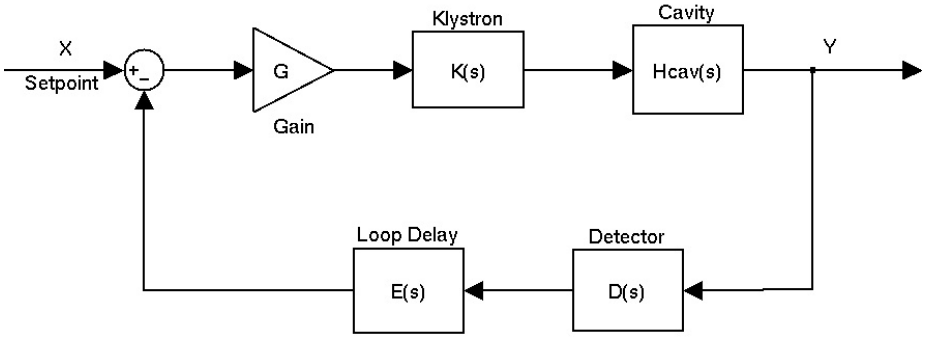

Figure 2: Block diagram of simplified the feedback control loop

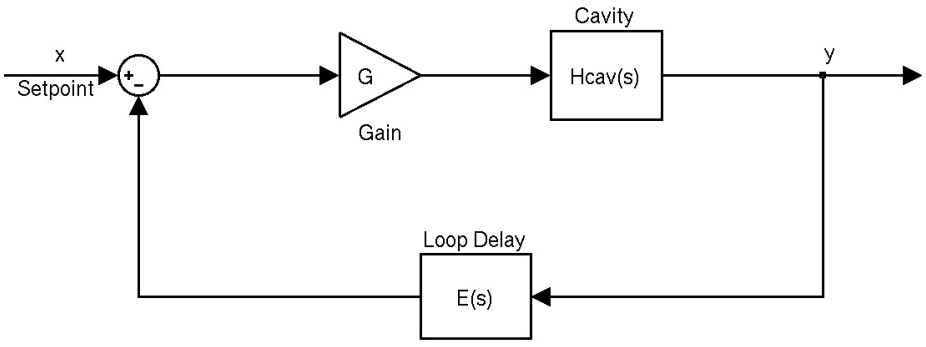

Figure 3: Block diagram of further simplified feedback control loop

The cavity behaviours like a low pass filter to phase and amplitude in the simplified control loop without considering Lorentz detuning and synchronous phase operation. Its transfer function can be written as [9]:

$$H_{cav}(f) = \frac{f_{hbw}}{jf + f_{hbw}}, \tag{10}$$

where f is the frequency variable, and f_{hbw} is the cavity half bandwidth .

The open loop transfer function $H_o(f)$ of the control loop in Figure 3 has the expressions as shown in Equations 11, 12, and 13, assuming that the bandwidths of the klystron and LLRF detector are both larger enough than the cavity bandwidth.

$$H_o(f) = GH_{cav}e^{-j2\pi\tau f}, \tag{11}$$

$$|H_o(f)| = \frac{G}{\sqrt{\left(\frac{f}{f_{hbw}}\right)^2 + 1}}, \tag{12}$$

$$\varphi = \angle H_o(f) = -\arctan\left(\frac{f}{f_{hbw}}\right) - 2\pi\tau f. \tag{13}$$

When $f \gg f_{hbw}$, the last two equations can be approximately written as:

$$|H_o(f)| = G\frac{f_{hbw}}{f}, \tag{14}$$

$$\varphi = -\frac{\pi}{2} - 2\pi\tau f. \tag{15}$$

Instability of the closed loop can be concluded from the characteristics of open loop transfer function, which occurs when the magnitude and the phase angle of the open loop transfer function are under special conditions as follows:

$$|H_o(f)| \geq 1, \tag{16}$$

$$\varphi = -\pi + n \cdot 2\pi, \quad n = 0, \pm 1, \pm 2, ... \tag{17}$$

Combining the Equation 14, 15, 16 and 17, we can calculate the critical frequency where the phase equals $-180°(-\pi)$ and the critical loop gain where the magnitude equals 0 dB. The lower the delay is, the higher the critical loop gain will be. Consequently the better feedback performance could be achieved. The critical loop gains obtained under different loop delays are listed in Table 2 both for superconducting cavity (with half bandwidth of 518 Hz, the current design value for ESS high beta cavity) and normal conducting cavity (assuming half bandwidth of 10 kHz).

The loop delay τ is set to 2µs in the following sections, which is the reasonable value considering the complicated perturbation factors (ripple, Lorentz detuning, passband modes, etc.), even though 1µs loop delay is achieved in some cavities at SNS (but some cavities are still larger than 1µs, even up to 1.5µs). At 2 µs loop delay, the critical gains are 241 and 12 for superconducting cavity and normal conducting cavity respectively, and the critical frequency is 125kHz for both.

It is at risk to have loop gain below but close to the critical gain, which causes overshoot as shown in Figures 4 and 5. We can see clearly from the figures that the loop gain around 0.3G (G is the critical gain)

Table 2: Critical loop gains obtained under different loop delays

	Superconducting cavity		Normal conducting cavity	
Delay/us	HBW/Hz	Critical gain	HBW/Hz	Critical gain
1	518	482	10000	25
1.5	518	321	10000	16
2	518	241	10000	12
2.5	518	193	10000	10
3	518	160	10000	8

is smooth enough without overshoot, which means the loop gain of 72 for superconducting cavity and 4 for normal conducting cavity. In practice, at SNS the average loop gain is about 50 for superconducting cavity and 6 for normal conducting cavity [6, 11]. In JPRAC where only the normal conducting cavities are used the average loop gain is about 5 [12]. In FLASH, the loop gain is about $70 \sim 100$ [9, 13].

3.2 Suppression of the klystron output variation by proportional gain

The influence of the ripple and droop of the modulator on klystron is equivalent to adding a noise to the klystron output. The block diagram of the feedback loop with noise is given in Figure 6, which is applicable for both phase and amplitude loops (or I &Q loops). The noise inside the cavity bandwidth is fully passed to the cavity in open loop via the path from r to y, while suppressed by a factor of G+1 (G is the loop gain) in closed loop, as shown in Figure 7.

The larger the loop gain, the better the loop performance against noise. The characteristics are shown obviously in Figures 8 and 9. However, it is also found that larger gain induces bigger overshoot and longer oscillation.

With only the proportional controller, it is hard for the normal conducting cavity to deal with large perturbation (with a loop gain of 6, for example, a perturbation of 15° phase variation can be only suppressed to 2.5°). What's worse, it leaves big steady error as seen from Figure 4. These are the reasons why the integral controller needs to be introduced as well in the feedback control.

3.3 Suppression of the klystron output noise by proportional-integral controller

As mentioned above, to eliminate the steady error and better suppress the noise, apart from the proportional controller we also have to employ the integral controller. The larger the integral gain is, the better the noise suppression performance of the integral controller will be at low frequency. However, larger integral gain consumes more phase margin, thereby increasing the risk of raising the instability.

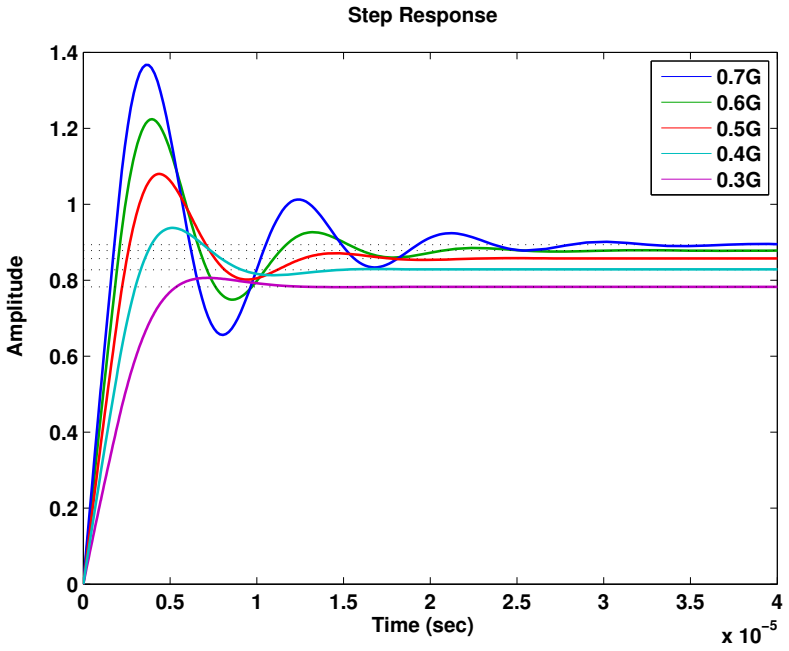

Figure 4: The step response of feedback for normal conducting cavity(G=12)

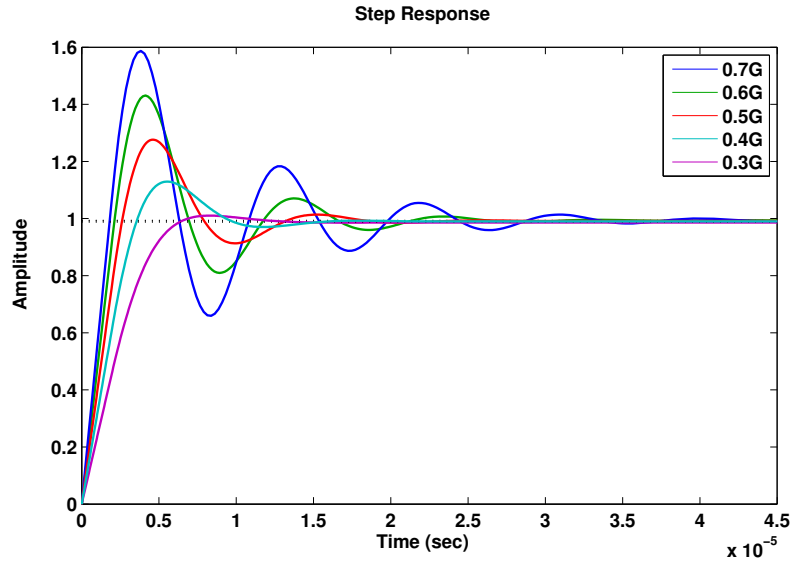

Figure 5: The step response of feedback for superconducting cavity(G=241)

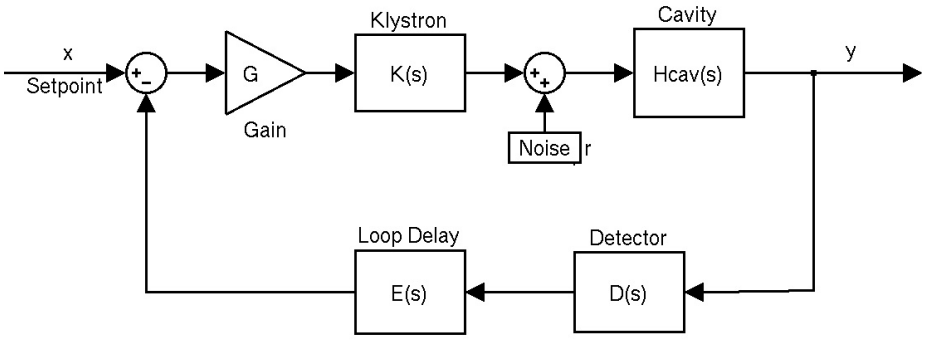

Figure 6: Block diagram of the proportional control feedback loop with noise

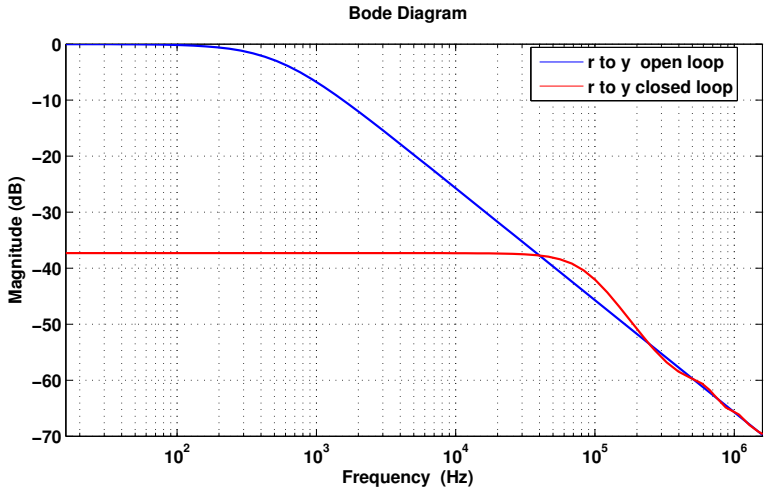

Figure 7: Noise suppression performance of the open loop and closed loop for proportional feedback control (Loop gain: G=72)

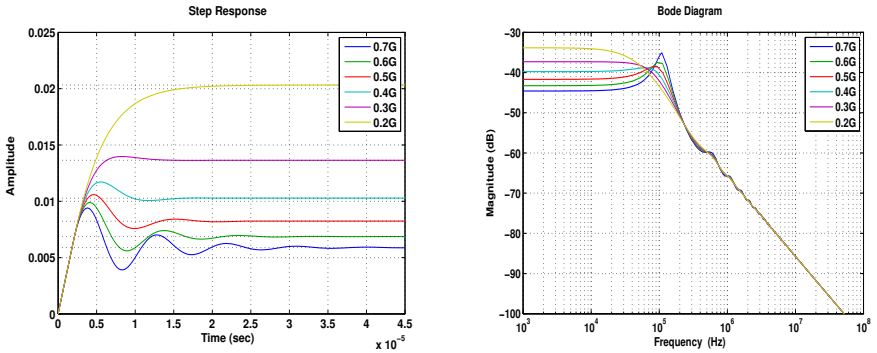

Figure 8: Closed loop noise suppression for superconducting cavity(G=241)

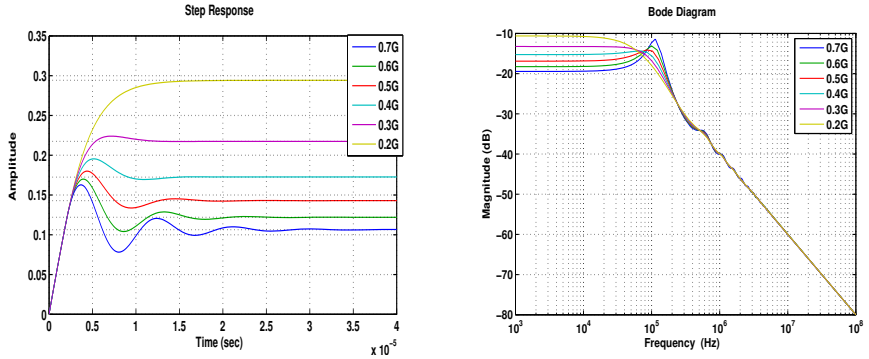

Figure 9: Closed loop noise suppression for normal conducting cavity(G=12)

The block diagram of the feedback loop with PI (proportional-integral) controller [14] is given in Figure 10, where Kp is the proportional gain and Ki is the integral gain. In the feedback loop with PI controller, the open loop transfer function can be written as:

$$\begin{aligned} H_o(f) &= K_p\left(1+\frac{K_i}{j2\pi f}\right)H_{cav}(f)\,e^{-j2\pi\tau f} \\ &= K_p\left(\frac{j2\pi f+K_i}{j2\pi f}\right)\left(\frac{f_{hbw}}{jf+f_{hbw}}\right)e^{-j\pi\tau f}, \end{aligned} \tag{18}$$

$$|H_o(f)| = K_p\sqrt{1+\left(\frac{K_i}{2\pi f}\right)^2}\Big/\sqrt{1+\left(\frac{f}{f_{hbw}}\right)^2}, \tag{19}$$

$$\varphi = \angle H_o(f) = \arctan\left(\frac{2\pi f}{K_i}\right) - \arctan\left(\frac{f}{f_{hbw}}\right) - \frac{\pi}{2} - 2\pi\tau f. \tag{20}$$

We firstly consider the case without loop delay (τ is 0). It is obviously seen from Equation 20 that when $\arctan\left(\frac{2\pi f}{K_i}\right) > \arctan\left(\frac{f}{f_{hbw}}\right)$, i.e., $K_i < f_{hbw}$, the loop phase is always larger than -90° ($-\pi/2$), which means there is

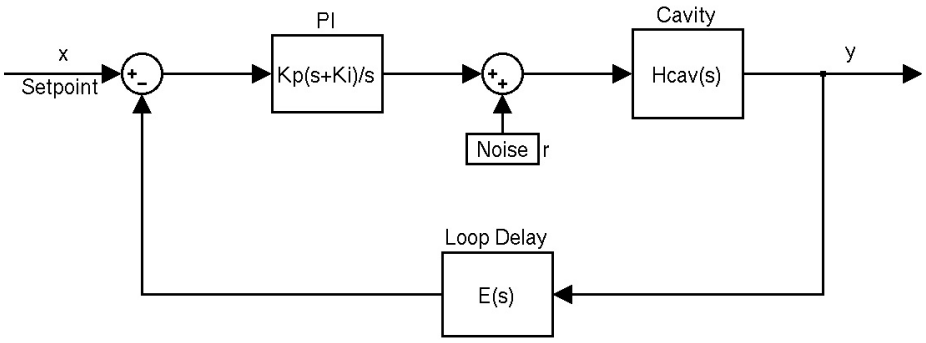

Figure 10: Block diagram of the feedback loop with PI controller

enough phase margin away from instability point (−180°). On the other hand, the phase margin will be less and less if integral gain continues increasing above $2\pi f_{hbw}$. It can be seen clearly in the bode diagram of open loop as shown in Figure 11. What's worse is that there exists delay in the loop, which makes the feedback control with large integral gain vulnerable to causing instability. Figure 12 shows the case with 2μs delay, in which the instability arises inevitably as the integral gain becomes larger and larger. In practice, the integral gain is set to $2\pi f_{hbw}$ so as to keep a constant loop phase and larger phase margin at all frequencies.

Having set the proper proportional and integral gains, it is able to look into the closed loop performance against the noise. The proportional gains of Kp=6 for normal conducting cavity and 50 for superconducting cavity, and the integral gain of $K_i = 2\pi f_{hbw}$ are firstly taken as analyzed above. The noise suppressions in closed loops as a function of frequency are given in Figures 13 and 14 for superconducting cavity and normal conducting cavity separately.

It is found from Figures 13 and 14 that with integral controller the feedback loop can suppress effectively the low frequency noise but the performance degrades as frequency increases, while the far higher frequency noise is filtered by cavity itself. Assuming that 15° phase variation is induced by per 1% change of the cathode voltage, and 0.5° phase variation is to be achieved under feedback control, we can obtain the noise tolerance as listed in Tables 3 and 4. For the modulator ripple, the trouble frequencies are usually less than hundred kHz. It is therefore valuable for us to focus on the rising part of the curves in figures above and the corresponding results in tables.

Tables 3 and 4 indicate that for a ripple of 3% in cathode voltage, the ripple frequency must be limited to less than several hundred Hz in order to achieve the required phase variation for superconducting and normal conducting cavities, and for a 1% ripple, the frequency has to be less than a couple of kHz for normal conducting cavity. Superconducting cavity feedback loop has much better performance against noise at higher frequency due to its intrinsic ability to achieve higher proportional gain. As there exists other factors affecting the feedback performance such as

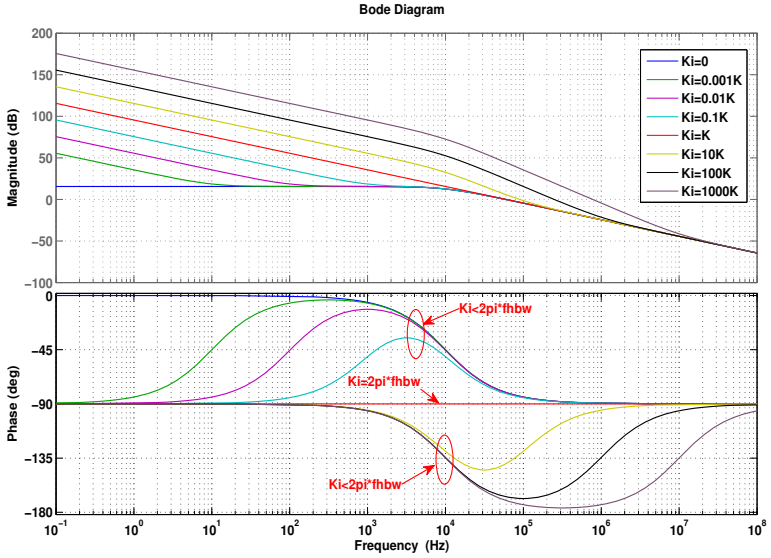

Figure 11: Phase margin reduced in open loop under different integral gains (without delay, $K = 2\pi f_{hbw}$)

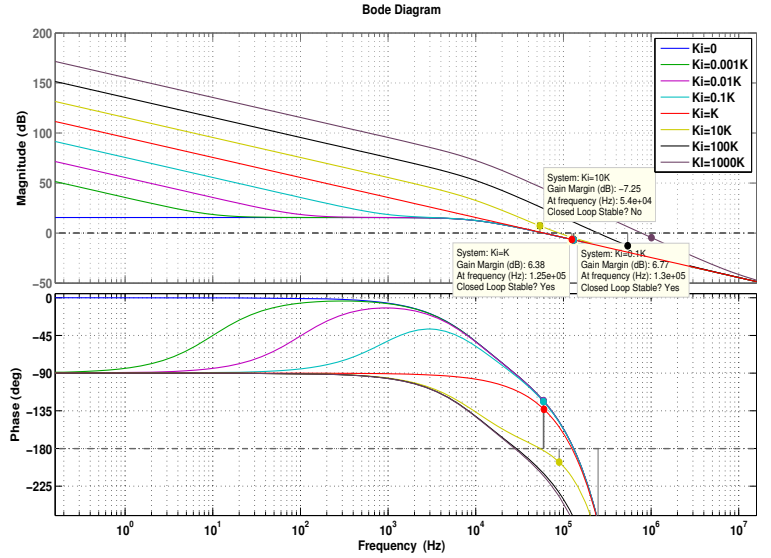

Figure 12: Phase margin reduced in open loop under different integral gains (2µs delay, $K = 2\pi f_{hbw}$)

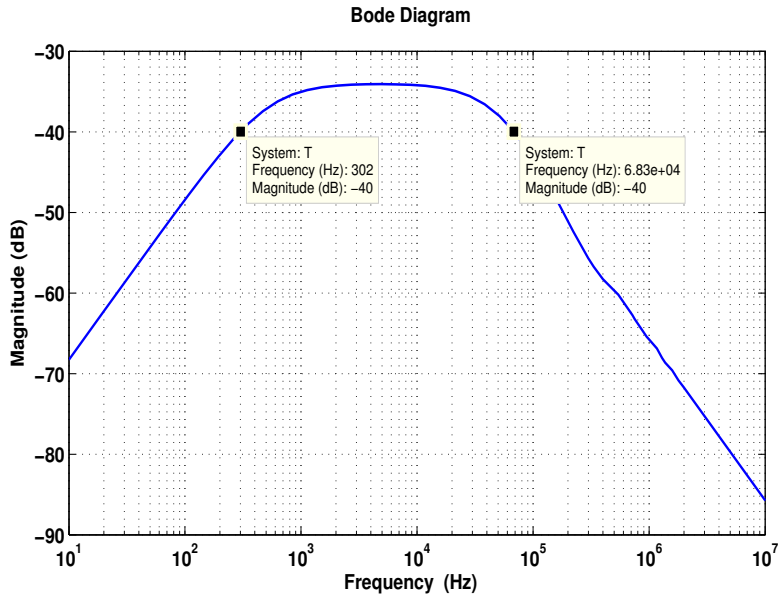

Figure 13: Noise suppression performance of PI feedback closed loop as a function of frequency for superconducting cavity($K_p = 50, K_i = 2\pi \times 518$)

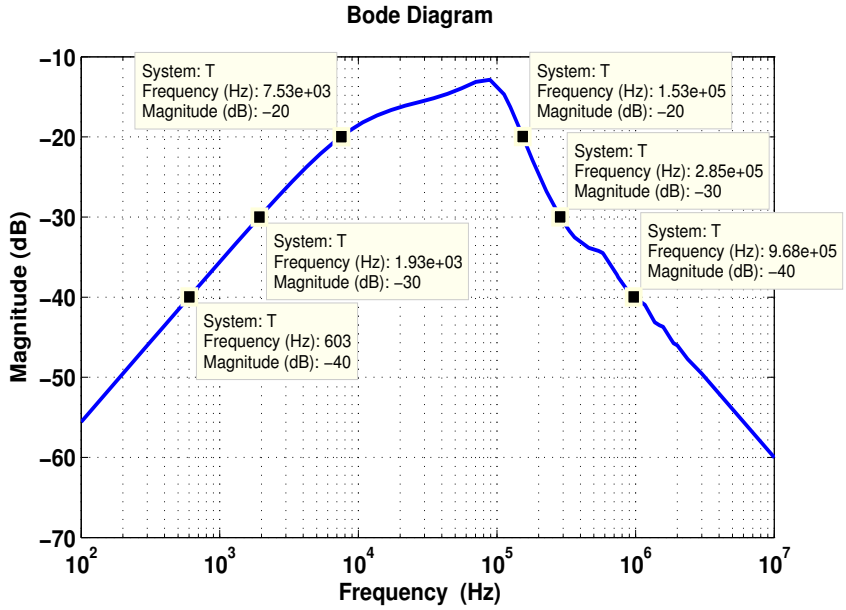

Figure 14: Noise suppression performance of PI feedback closed loop as a function of frequency for normal conducting cavity($K_p = 6, K_i = 2\pi \times 10^4$)

Table 3: Noise tolerances of PI feedback closed loop at different frequencies (Superconducting cavity, $K_p = 50, K_i = 2\pi \times 518$)

Frequency range /kHz	Gain available	Tolerance in output phase/°	Tolerance in cathode voltage
<0.3, or >68	>100	>50	>3.3%
0.3 ~ 68	50 ~ 100	25 ~ 50	1.7% ~ 3.3%

Table 4: Noise tolerances of PI feedback closed loop at different frequencies (Normal conducting cavity, $K_p = 6, K_i = 2\pi \times 10^4$)

Frequency range /kHz	Gain available	Tolerance in output phase/°	Tolerance in cathode voltage
<0.6, or >97	>100	>50	>3.3%
0.6 ~ 2, 280 ~ 970	30 ~ 100	15 ~ 50	1% ~ 3.3%
2 ~ 7.5, 150 ~ 280	10 ~ 30	5 ~ 15	0.33% ~ 1%
7.5 ~ 150	4.5 ~ 10	2.25 ~ 5	0.15% ~ 0.33%

unpredicted noise, cavity detuning and passband modes, the performance of PI feedback against noise might degrade. A much worse case of proportional gain of 20 for superconducting cavity and 1 for normal conducting cavity is shown in Figures 15, 16 and Tables 5, 6. In both superconducting and normal conducting cavities, the frequency is limited to less than 100 Hz for 3% ripple, while less than several hundred Hz is needed for 1% ripple. Normal conducting cavity feedback loop has a poorer performance for the frequencies of higher than 1 kHz, at which the ripple should be limited to the order of 0.1%.

In considering both cases above, to control the phase variation within 0.5°, it therefore seems better to keep the modulator ripple <1% at low frequency (<1 kHz), while <0.1% for normal conducting cavity and <0.5% for superconducting cavity at higher frequency (>1 kHz). For the ripple with frequency below 100 Hz, it is able to leave the ripple at around 3% or even higher for much lower frequencies.

The modulator droop can be seen as very low frequency ripple or even DC component noise in feedback loop, and therefore theoretically the droop could be larger than 3% in cathode voltage. However, larger droop or ripple will consume more power and reduce phase adjustment range of the feedback loop. For example, around 8% more power and 45 ° in phase (assuming 15° is induced by per 1% variation in cathode voltage) are needed to compensate 3% droop in feedback loop, while 13% more power and 75° in phase are needed for 5% droop. For the purpose of power efficiency and achievement of good feedback performance, it is necessary to reduce the droop and ripple as much as possible.

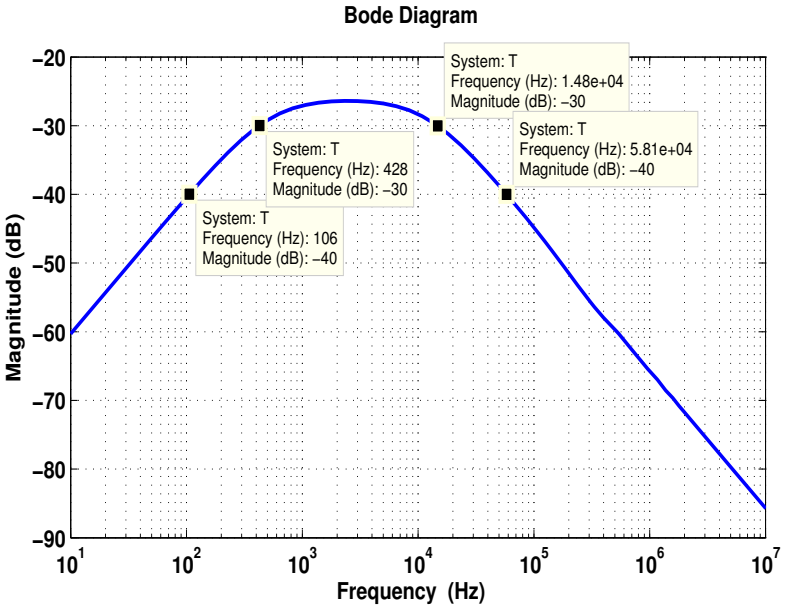

Figure 15: Noise suppression performance of PI feedback closed loop as a function of frequency for superconducting cavity($K_p = 20, K_i = 2\pi \times 518$)

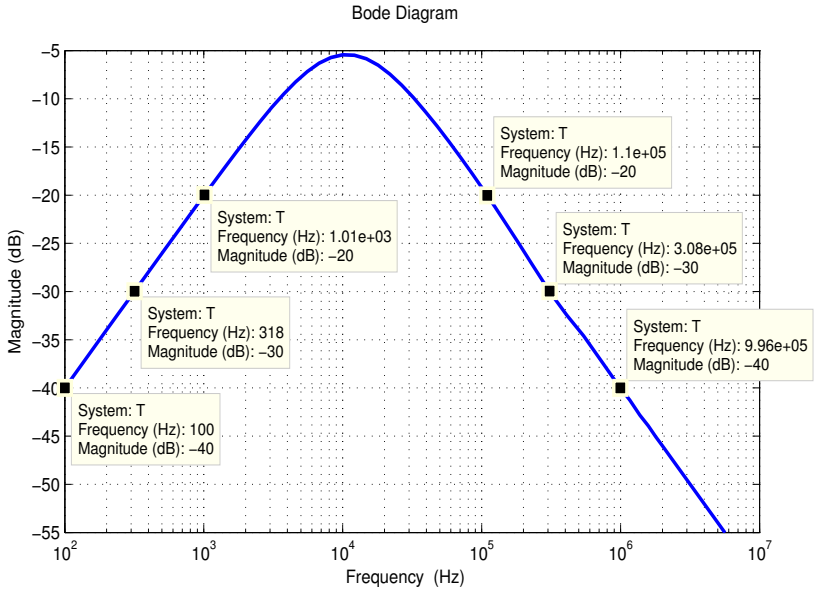

Figure 16: Noise suppression performance of PI feedback closed loop as a function of frequency for normal conducting cavity($K_p = 1, K_i = 2\pi \times 10^4$)

Table 5: Noise tolerances of PI feedback closed loop at different frequencies (Superconducting cavity, $K_p = 20, K_i = 2\pi \times 518$)

Frequency range /kHz	Gain available	Tolerance in output phase/°	Tolerance in cathode voltage
<0.1, or >58	>100	>50	>3.3%
0.1 ~ 0.4, 15 ~ 58	30 ~ 100	15 ~ 50	1% ~ 3.3%
0.4 ~ 15	20 ~ 30	10 ~ 15	0.7% ~ 1%

Table 6: Noise tolerances of PI feedback closed loop at different frequencies (Normal conducting cavity, $K_p = 1, K_i = 2\pi \times 10^4$)

Frequency range /kHz	Gain available	Tolerance in output phase/°	Tolerance in cathode voltage
<0.1, or > 1000	>100	>50	>3.3%
0.1˜0.3, 300˜1000	30 ~ 100	15 ~ 50	1% ~ 3.3%
0.3 ~ 1, 100 ~ 300	10 ~ 30	5 ~ 15	0.33% ~ 1%
1 ~ 100	2 ~ 10	1 ~ 5	0.07% ~ 0.33%

4 Conclusion

The modulator droop and ripple of per 1% induces more than 10° in klystron output phase and 1.25% in amplitude (2.5% in power). The PI feedback loop has trouble to deal with the noises with high amplitude and high frequency due to loop delay and the necessity to keep proper phase margin. It would be better to keep the modulator droop and ripple <1% in low frequency range (<1 kHz), while <0.1% for normal conducting cavity and <0.5% for superconducting cavity in higher frequency range (>1 kHz). For the modulator droop and very low frequency ripple below 100 Hz, the tolerance for the ripple could be up to 3% or even higher, but it consumes more power and more phase dynamic range. It is essential to reduce the droop and ripple as much as possible.

References

[1] http://www.radartutorial.eu/08.transmitters/tx12.en.html.

[2] M. Hara, T. Nakamura, and T. Ohshima. A Ripple Effect of a Klystron Power Supply on Synchrotron Oscillation. *Particle Accelerators*, 59(3):143–156, 1998.

[3] Jr. A.S.Gilmour. *Klystrons, Traveling Wave Tubes, Magnetrons, Crossed-Field Amplifiers, and Gyrotrons*, chapter Nonlinearities and Distrotion. Artech House, 2011.

[4] T. Kobayashi, E. Chishiro, T. Hori, H. Suzuki, M. Yamazaki, S. Anami, Z. Fang, Y. Fukui, M. Kawamura, and S.Michizono. Performance of J-PARC linac RF system. In *Particle Accelerator Conference, 2007. PAC. IEEE*, pages 2128–2130, 2007.

[5] M. McCarthy, M. Crofford, and S. K ORNL. Spallation neutron source superconducting linac klystron to cavity mismatch effects and compensation. In *Proceedings of the 2008 Linear Accelerator Conference*, 2008.

[6] B. Chase and M. Champion. SNS LLRF Design Experience and its Possible Adoption for the ILC. International Linear Collider Workshop, 2005.

[7] P. Corredoura, R. Claus, L. Sapozhnikov, H. Schwarz, R. Tighe, and C. Ziomek. Low level RF system design for the PEP-II b factory. In *Particle Accelerator Conference, 2002*, volume 4, pages 2672–2674, 2002.

[8] S. Chel, M. Desmons, A. Hamdi, and F. Peauger. New 1 MW 704 MHz RF test stand at CEA-Saclay. *Proc. EPAC08*, 2008.

[9] M. Hoffmann. *Development of a multichannel RF field detector for the Low-Level RF control of the Free-Electron Laser at Hamburg*. PhD thesis, Hamburg University of Technology, 2008.

[10] T. Schilcher. *Vector Sum Control of Pulsed Accelerating Fields in Lorentz Force Detuned Superconducting Cavities*. PhD thesis, University of Hamburg, 1998.

[11] Hengjie Ma, Mark Champion, Mark Crofford, Kay-Uwe Kasemir, Maurice Piller, Lawrence Doolittle, and Alex Ratti. Low-level rf control of spallation neutron source: System and characterization. *Phys. Rev. ST Accel. Beams*, 9(3):032001, Mar 2006.

[12] S. Michizono, S. Anami, M. Kawamura, S. Yamaguchi, and T. Kobayashi. Digital rf control system for 400-mev proton linac of jaeri/kek joint project. In *Proceedings of the 2002 Linear Accelerator Conference*, 2002.

[13] V. Ayvazyan, S. Choroba, Z. Geng, G. Petrosyan, S. Simrock, and D. Vladimir Vogel. OPTIMIZATION OF FILLING PROCEDURE FOR TESLA-TYPE CAVITIES FOR KLYSTRON RF POWER MINIMIZATION FOR EUROPEAN XFEL. In *Proceedings of 1st International Particle Accelerator Conference: IPAC'10*, 2010.

[14] Sung il Kwon, Joseph Bradley, Amy Regan, Yi-Ming Wang, and Tony Rohlev. SNS MODELING - HIGH VOLTAGE POWER SUPPLY RIPPLE ANALYSIS. Technical report, Los Alamos National Laboratory, 2000.

A Phase variation due to cathode voltage change in relativistic case

$$(\gamma - 1)\, mc^2 = eV \tag{21}$$

$$\gamma = \frac{eV}{mc^2} + 1 \tag{22}$$

$$\beta = \sqrt{1 - \frac{1}{\gamma^2}} \tag{23}$$

$$t = \frac{L}{\upsilon} = \frac{L}{c\beta} \tag{24}$$

$$\theta = \omega t = \frac{\omega L}{c\beta} \tag{25}$$

$$\frac{d\theta}{d\beta} = -\frac{\omega L}{c\beta^2} \tag{26}$$

$$\frac{d\beta}{d\gamma} = \frac{1}{2\sqrt{1 - \frac{1}{\gamma^2}}} \cdot \frac{2}{\gamma^3} = \frac{1}{\beta\gamma^3} \tag{27}$$

$$\frac{d\gamma}{dV} = \frac{e}{mc^2} \tag{28}$$

$$\frac{d\theta}{dV} = \frac{d\theta}{d\beta}\frac{d\beta}{d\gamma}\frac{d\gamma}{dV} = -\frac{e\omega L}{mc^3\beta^3\gamma^3} \tag{29}$$

$$d\theta = -\frac{e\omega LV}{mc^3\beta^3\gamma^3} \cdot \frac{dV}{V} \tag{30}$$

B Superconducting cavity feedback performance with low proportional gain

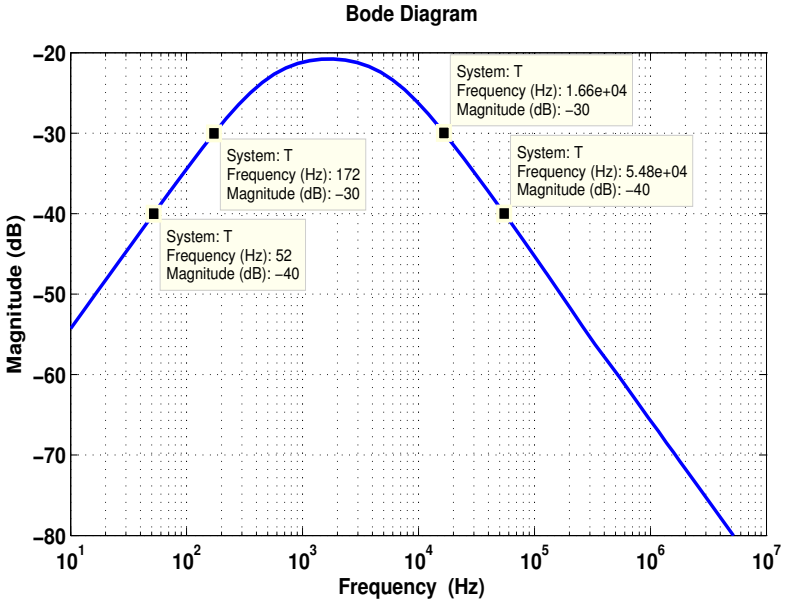

Figure 17: Noise suppression by feedback closed loop($K_p = 10, K_i = 2\pi \times 518$)

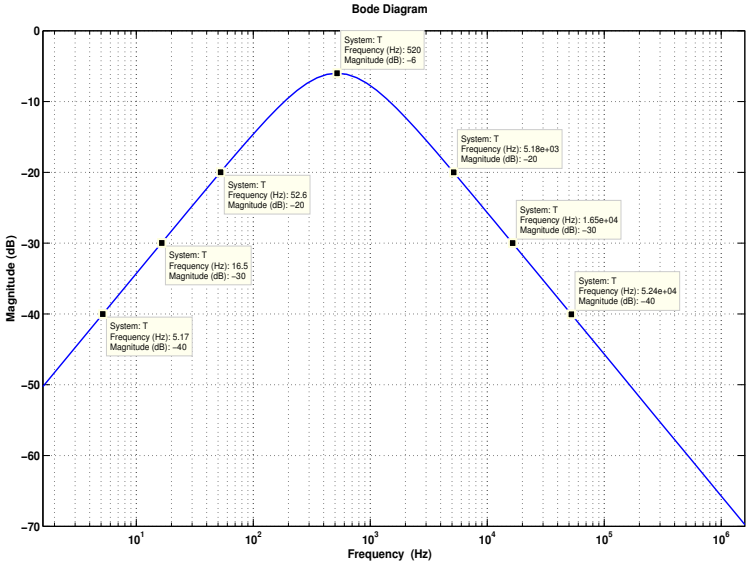

Figure 18: Noise suppression by PI feedback closed loop($K_p = 1, K_i = 2\pi \times 518$)